

Thermoelectric effects in nanostructured quantum wires in the non-linear temperature regime

Anda Elena Stanciu¹, G. A. Nemnes^{1,2}, and A. Manolescu³

¹*University of Bucharest, Faculty of Physics, Materials and Devices for Electronics and Optoelectronics Research Center, 077125 Magurele-Ilfov, Romania*

²*Horia Hulubei National Institute for Physics and Nuclear Engineering, 077126 Magurele-Ilfov, Romania*

³*School of Science and Engineering, Reykjavik University, Menntavegur 1, IS-101 Reykjavik, Iceland*

Abstract

The thermoelectric voltage of a quantum dot connected to leads is calculated using the scattering R-matrix method. Our approach takes into account a temperature gradient between the contacts beyond the linear regime. We obtain sign changes of the thermopower when varying the temperature or the chemical potential around the resonances. The influence of the coupling strength of the contacts and of the thermoelectric field on the thermoelectric voltage is discussed.

Keywords: thermoelectrics, R-matrix, non-linear temperature regime.

1 INTRODUCTION

The history of nanoscale thermoelectrics dates back to the 90's when it was shown that quantum wires and quantum wells may provide an enhancement of the figure of merit compared to the calculated value for the bulk structures [1]. Since then, studies on various quantum systems have been performed, and especially on thermoelectric efficiency [2, 3, 4, 5]. Small diameter nanowires [6, 7] as well as quantum dot systems [8] investigated from both theoretical and experimental point of view provide special thermoelectric characteristics as they present sharp features [9] in the transmission functions. The nonlinear temperature regime offers new ways to obtain an enhanced thermoelectric efficiency. In this study we analyze thermoelectric effects which arise due to a temperature difference between the contacts of a device model using the scattering formalism based on the R-matrix. We present the typical features observed in resonant systems [10], such as the sign-change of the thermoelectric voltage by changing the chemical potential around and in-between the resonances [11, 12], but also by varying the temperature of the contacts. The influence of the coupling between the quantum system and the contacts is analyzed. Finally, the non-linear effects introduced by the thermoelectric field between the contacts

are incorporated and the possible enhancement of the thermoelectric voltage is discussed.

2 Model and method

The two-terminal model device is a double barrier system as illustrated in Fig. 1. The leads are invariant along the transport direction and the perpendicular confinement is parabolic, with a level spacing $h\omega_0 = 100$ meV. The contacts have distinct temperatures T_1 and T_2 .

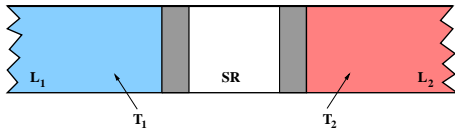


Figure 1: Schematic representation of the two-dimensional system composed by the two leads and the scattering region SR. The gray areas are potential barriers which describe the couplings between SR and the two leads $L_{1,2}$ which have different temperatures, $T_2 > T_1$.

In the framework of multi-channel coherent transport [7, 13, 14], the transmission function is calculated as

$$\mathcal{T}_{ss'}(E) = \sum_{i,i'} \Theta(E - E_{\perp}^{\nu}) \Theta(E - E_{\perp}^{\nu'}) \left| \tilde{S}_{\nu\nu'}(E) \right|^2, \quad (1)$$

where $\nu = (s, i)$ denotes the channel index i in lead s ($s = 1, 2$) and $\tilde{S} = K^{\frac{1}{2}} S K^{-\frac{1}{2}}$. The diagonal matrix K is formed by longitudinal wavevectors, $k_{\nu} = \sqrt{2m(E - E_{\perp}^{\nu})}/\hbar$, where E_{\perp}^{ν} is the transversal energy for channel ν and E is the total energy. The scattering S-matrix is found in the R-matrix method as $S = -(1 + \frac{i}{m^*} RK)/(1 - \frac{i}{m^*} RK)$. By using the Heaviside functions Θ in Eq. (1) only the open channels are included. The current is calculated as:

$$I \equiv I_{ss'} = \frac{2e}{h} \int dE \mathcal{T}_{ss'}(E) [f_{FD}(E; \mu_1, T_1) - f_{FD}(E; \mu_2, T_2)], \quad (2)$$

where $f_{FD}(E; \mu, T)$ is the Fermi-Dirac distribution function. The open circuit thermoelectric voltage U_{th} produced by the temperature difference $\Delta T = T_2 - T_1$ is found by imposing a vanishing current condition, $I = 0$. The value U_{th} is determined iteratively, by changing step-wise the relative positions of the chemical potentials, which in turn modify the internal electric field between the contacts and the scattering potential as well.

3 Results

We use rectangular barriers of height $V_b = 200$ meV and width $w = 4.3$ nm. The distance between the contacts, including the barriers, is $L = 46$ nm. The effective mass of the electron is as for InAs, $m^* = 0.023m_e$. We consider $T_1 = 0$, but $T_2 \neq 0$.

We first examine the influence of the coupling of the resonant system with the contacts by adjusting the widths of the barriers. The transmission functions are depicted in Fig. 2(a), for the system with the specified barrier width

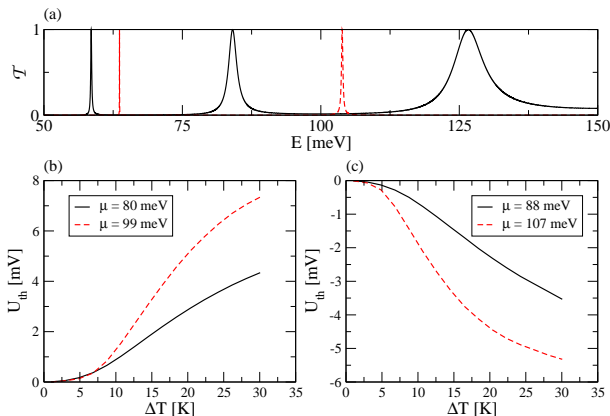


Figure 2: (a) The transmission functions for systems with barrier widths $w = 4.3$ nm (black/solid) and $2w$ (red/dashed). Thermoelectric voltage vs. temperature difference, with the chemical potential at zero bias μ chosen below (b) and above (c) the energy of the second resonance peak.

w , and, for comparison, for $2w$. By doubling the barrier width the coupling to the leads weakens and the energy levels are shifted at higher energies while the transmission peaks become narrower. For each system we consider two values for the chemical potential, one placed below and one above the second resonant level E_2^{res} . The thermoelectric voltage as a function of temperature difference is presented in Figs. 2(b) and (c). In order to compare the effects produced by the resonance broadening rather than energy shift, the initial chemical potentials of the leads, i. e. at zero bias, denoted by μ , are chosen symmetrically, on both sides of the transmission maximum of the second resonance peak. The thermoelectric voltage is calculated as $U_{th} = (\mu_1 - \mu_2)/|e|$, $\mu_{1,2}$ being the chemical potentials of the leads, where $\mu_2 = \mu$ is fixed and μ_1 is adjusted until the current generated by the temperature gradient vanishes.

Two main features are observed. First, the sign of U_{th} changes as the chemical potential is situated above or under the resonant level. This indicates that the thermoelectric current generated at zero bias has changed sign. Second, the weaker coupling, leading to narrower transmission peaks, corresponds to an enhanced $|U_{th}|$. The behavior can be explained as follows: in the limit of narrow peaks, the condition $I = 0$ is fulfilled as the position of the chemical potential in the cold contact, μ_1 , reaches the resonant level, E_2^{res} , and the populations in the two contacts become equal; if the resonance is broader the vanishing current condition is reached sooner as μ_1 is shifted towards E_2^{res} , leading to smaller $|U_{th}|$.

Next, for the system with barrier width of 4.3 nm the zero-bias chemical potential is varied around the first resonance and also between the first two resonances. The two resonances occur at $E = 58$ and $E = 84$ meV, Fig. 1(a). The results are shown in Figs. 3(a) and (b). In the first case the voltage curves have intersections at finite temperatures. At temperatures below the intersections $|U_{th}|$ increases as the chemical potential is set closer to the resonance maximum and at higher temperatures the opposite situation occurs. This is a consequence of the overlap of the Fermi-Dirac distribution functions with the finite width of

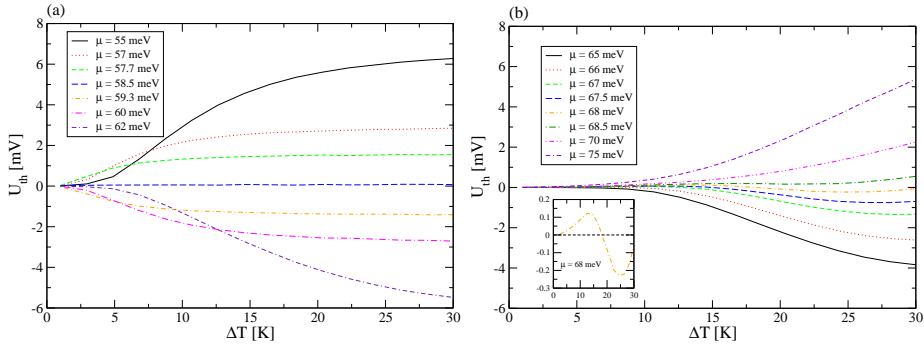


Figure 3: Thermoelectric voltage vs. temperature difference: chemical potential varying around the first resonance (a) and in-between the first two resonances (b). Inset: sign change of U_{th} at a fixed μ .

the resonance. In the second case, one also obtains a sign change for U_{th} at a fixed temperature, because by changing the chemical potential one out of the two resonances becomes dominant. Moreover, the same effect is also found at a fixed chemical potential and variable temperature, as one can see in the inset of Fig. 3(b).

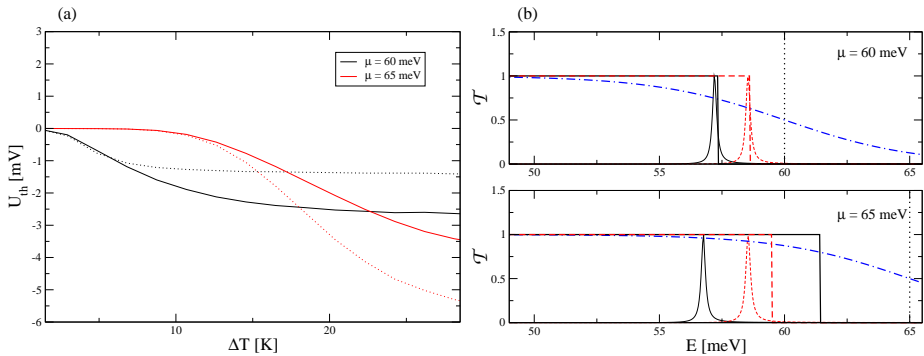


Figure 4: (a) U_{th} vs. ΔT in the presence of the thermoelectric field (solid lines) and in the absence of the thermoelectric field (dotted lines). (b) Transmission functions and populations in contact 1 for the case *with* (black/solid) and *without* (red/dashed) thermoelectric fields, at $\Delta T = 30$ K. The populations in contact 2 are represented by (blue/dot-dashed) lines.

The thermoelectric fields arising between the contacts $\mathcal{E}_{th} = U_{th}/L$ constitute a source of non-linear behavior and possible enhancement of the thermoelectric effects. Numerical results are shown in Fig. 4(a) to compare the case *with* and *without* \mathcal{E}_{th} included in the transmission function given by Eq. 1. The chemical potentials are selected in-between the first two resonances for $w = 4.3$ nm. We find that if the chemical potential is close to the resonance the inclusion of \mathcal{E}_{th} enhances $|U_{th}|$, whereas if μ is farther away the opposite is true. The situation is illustrated in Fig. 4(b) for two values of the chemical potential. In the presence of the thermoelectric field the resonant levels are shifted in the same direction as the chemical potential μ_1 . At $\Delta T = 30$ K, for $\mu = 60$ meV this

produces an increase of $|U_{th}|$. However, if we set $\mu = 65$ meV, the population at the resonance is larger and the positions of μ_1 for the cases *with* and *without* \mathcal{E}_{th} become reversed and $|U_{th}|$ decreases.

4 Conclusions

The thermoelectric effects which arise in the non-linear temperature regime in a multi-resonance system were discussed in the framework of coherent transport, using a scattering formalism based on the R-matrix method. We point out the typical features of sign changing of the thermoelectric voltage with respect to varying the chemical potential around a resonance and in-between two consecutive resonances. In the latter case, this sign change is also obtained by modifying the temperature difference at a fixed chemical potential. This effect is shown in the recent Ref. [15] in the presence of Coulomb interaction of electrons, whereas we could obtain it without interactions. Furthermore, we discussed the conditions for enhancing the thermoelectric effect in the non-linear regime.

Acknowledgement

Support of the EEA Financial Mechanism 2009-2014 staff mobility grant and the hospitality of Reykjavik University are gratefully acknowledged. G. A. Nemnes also acknowledges support from ANCS under grant PN-II-ID-PCE-2011-3-0960.

References

- [1] L. D. Hicks, M. S. Dresselhaus, Phys. Rev. B **47**, 16631(R) and 12727 (1993).
- [2] T. E. Humphrey, H. Linke, Phys. Rev. Lett. **94**, 096601 (2005).
- [3] B. Sothmann, R. Sánchez, A. N. Jordan, M. Büttiker, New J. Phys. **15**, 095021 (2013).
- [4] M. F. O'Dwyer, T. E. Humphrey, H. Linke, Nanotechnology **17**(11), S338 (2006).
- [5] O. Karlström, H. Linke, G. Karlström, A. Wacker, Phys. Rev. B **84**, (2011).
- [6] J. P. Heremans, Acta Phys. Pol. A, **108**, 609 (2005).
- [7] G. A. Nemnes, L. Ion, S. Antohe, Physica E **42**, 1613 (2010).
- [8] S. F. Svensson et al., New J. Phys. **15**, 105011 (2013).
- [9] G. D. Mahan, J. O. Sofo, Appl. Phys. Sci., **93**, 7436 (1995).
- [10] Jianming Wang et al., Mod. Phys. Lett. B **20**, 215 (2006).
- [11] C. W. J. Beenakker and A. A. M. Staring, Phys. Rev. B **46**, 9667 (1992).
- [12] K. Torfason, A. Manolescu, S. I. Erlingsson, V. Gudmundsson, Physica E **53**, 178 (2013).
- [13] G. A. Nemnes, L. Ion, S. Antohe, J. Appl. Phys. **106**, 113714 (2009).
- [14] G. A. Nemnes, A. Manolescu, V. Gudmundsson, J. Phys.: Conf. Ser. **338**, 012012 (2012).
- [15] M. A. Sierra and D. Sanchez, Phys. Rev. B, **90**, 115313 (2014).